

¹Nang-Van Pham¹Van-Y Pham

Influence of Load Models and DG Operational Power Factor on Optimization of Shunt Capacitor Placement in Distribution Grids Considering Voltage Stability



Abstract: - The paper proposes a mathematical model of mixed-integer nonlinear programming (MINLP) to optimize the location and size of shunt capacitors in power distribution grids with distributed generation (DG), considering voltage stability constraints. At the same time, the paper also analyzes the influence of the load models, such as voltage-dependence load (ZIP load) and constant power load, together with DG's operating power factor on the optimal solution. The objective function of the proposed optimization formulation is minimizing the total expenses, including the capital investment of capacitors and the expense incurred by network energy loss. This MINLP model includes constraints in the current and critical loading conditions, such as the system of power flow equations, nodal voltage limits, branch thermal limits, capacitor-related constraints, and restrictions of minimum security level. The proposed optimization model was evaluated on a modified IEEE 33-node distribution grid using the KNITRO commercial solver with the GAMS programming language. The calculation results show that the voltage stability constraints, load models, and operational power factor of the DG units have an essential influence on the optimal position and capacity of the shunt capacitors.

Keywords: Distributed Generation (DG), Mixed-Integer Nonlinear Programming (MINLP), Power Distribution Grids, Shunt Capacitors, Voltage Stability, ZIP Load Model.

I. INTRODUCTION

The distributed generation (DG) widely penetrated into electrical distribution grids can alter the power flow and affect voltage stability [1]. The primary factor contributing to voltage instability is the insufficient availability of reactive power reserves. Voltage instability may result in voltage collapse, which can lead to extensive power outages and have a profound impact on the electrical system [2]. A viable solution to enhance the voltage stability of electrical power systems is the installation of devices such as shunt capacitors for compensating reactive power [3]. However, the efficiency of shunt capacitors is highly dependent on the choice of their location and capacity in the electrical power systems. Simultaneously, the power consumption model of the load and the operating mode of the on-site generators have a significant effect on the optimal investment of the shunt capacitors with the purpose of improving the voltage stability.

Recently, various contributions devoted to addressing the subject of optimizing the siting and sizing of shunt capacitors have been available in the technical literature. Authors [4] introduced a MINLP model to minimize the overall cost, including capacitor investment cost and power loss expenses. This proposed optimization model is evaluated on both radial distribution grids and mesh-structured distribution networks. However, the work [4] only considered the constant power load model. The MINLP approach based on the primal-dual interior point method combined with the Lagrange multiplier method to simultaneously optimize the grid topology and capacitor installation in the distribution systems was presented in [5]. However, voltage stability constraints were not taken into account in this study [5]. The Parallel Dual Tabu search method for optimally determining the capacitor allocation was demonstrated in [6]. This method is simple and easy to implement; however, some determinants, such as DG operating power factors, load model, and voltage stability constraints, are not dealt with. The authors [7] suggested a method on the basis of the Fuzzy Set Theory to select the optimal location and capacity of fixed capacitors in the distribution grids taking into account different harmonic conditions. The approach that combines the sensitivity analysis using the voltage stability index with a genetic algorithm (GA) with the aim of co-optimizing the allocation of capacitors and DG units was proposed in the work [8]. The goal function in [8] is to minimize power losses and enhance the quality of the nodal voltage profile. However, the effect of the load model has not been considered in [8]. The paper [9] demonstrated the particle swarm optimization (PSO)-based approach to select the optimal site and capacity of shunt capacitors in the power distribution grid. However, in the study [9], economic

¹School of Electrical and Electronic Engineering, Hanoi University of Science and Technology, Hanoi, Vietnam

*Corresponding author: Nang-Van Pham, E-mail: van.phamnang@hust.edu.vn

factors such as the expenses of capacitor investment and power losses were not addressed. The Harmony search algorithm (HSA) that takes the nonlinear loads into consideration to maximize the cost savings on losses when installing shunt capacitors was developed in [10]. The convergence of the method [10] is evaluated through the THD index of voltage, so the convergence rate may slow down when applied to large power grids. The Whale Optimization Algorithm (WOA) algorithm [11] was deployed to cope with the optimization problem with multiple objectives, including minimization of the total network power loss, minimization of the power loss-related expenses, and improvement of the voltage stability index. These objective functions are put together through the weighted sum method. Nevertheless, the study just examined situations where a predetermined quantity of capacitors were installed on the grid without taking into account the impact of the load model and operational attributes of the DG units on the placement and capacity of the shunt capacitor. Similarly, the paper [12] demonstrated the Turbulent Flow of the Waterbased Optimization Algorithm (TFWO) algorithm to optimize the site and quantity of various compensation devices in the power grid, including shunt capacitors, SVC, and DSTATCOM. The Artificial Neural Network (ANN) method in [13] was applied to determine capacitor switching in the distribution grid optimally. However, the limitation of this technique is the training time for large and complex power grids.

The works [4]-[13] did not consider the influence of the load model with voltage-dependent power consumption on the location and capacity of the installed shunt capacitors. However, the power distribution grids encompass many types of loads (residential, industrial, commercial), with electricity usage varying with the voltage magnitude. In order for the study to be more consistent with reality, the influence of the dependence of the power consumed by the load on the voltage on the optimal installation of shunt capacitors should be evaluated [14]. The Enhance Salps Swarm Algorithm (ESSA) approach, proposed in [15], aims to optimize the placement and rating of shunt capacitors in radial electrical distribution systems to address multiobjective functions. The PSO approach was applied in [16] to optimize the position of shunt capacitors in the radial power distribution grids, aiming at minimizing power losses. In addition, the impact of the operational power factor of the on-site generating units in the reactive power generation/consumption mode on the optimal siting and sizing of shunt capacitors should also be taken into account. Table 1 presents the studies in the literature related to the best location and rating of shunt capacitors in power distribution networks.

Table 1: Comparison of reported works in the literature and the model developed in this paper

Reference Number	Considering ZIP Load	Considering DG Units	Considering Voltage Stability	Objective Function	Solving Method
[4]	No	No	No	Capacitor cost and energy loss cost	MINLP
[5]	No	No	No	Energy loss cost	MINLP, Interior Point, Lagrange Multipliers
[6]	No	No	No	Capacitor cost and energy loss cost	Parallel Dual Tabu Search
[7]	No	No	No	Capacitor cost, power loss cost, and energy loss cost	Fuzzy Set Theory
[8]	No	Yes	Yes	Power loss	GA
[9]	No	No	No	Power loss	PSO
[10]	No	No	No	Capacitor cost and energy loss cost	HSA
[11]	No	No	No	Capacitor cost, power loss cost, and energy loss cost	WOA
[12]	No	No	No	Capacitor cost and power loss cost	TFWO
[13]	No	No	No	Energy loss cost	ANN
[14]	Yes	No	No	Power loss	MINLP

[15]	No	No	No	Power loss and total system cost	ESSA
[16]	No	No	No	Power loss	PSO
This paper	Yes	Yes	Yes	Capacitors cost and energy loss cost	MINLP

This paper aims to provide a mixed-integer nonlinear programming (MINLP) model that optimizes the placement and capacity of shunt capacitors in distribution grids with on-site generation. The model considers voltage stability restrictions and voltage-dependent loads (ZIP loads). This study has made critical contributions as follows:

- Suggest a Mixed-Integer Nonlinear Programming (MINLP) model for optimizing the placement and sizing of shunt capacitors. The target function is to minimize the overall cost, which includes the investment cost of the capacitors as well as the cost associated with energy loss in the network;
- Evaluate the effect of the minimum loading factor pertaining to the voltage stability constraint on the optimization of shunt capacitor placement;
- Evaluate the impact of distinct load models, such as constant power and ZIP loads, on the best location of shunt capacitors;
- Evaluate the impact of DG’s operational power factor on the optimal solution.

The subsequent sections of this work are organized as follows. Section II presents the MINLP model for optimizing the placement and capacity of shunt capacitors. This includes a detailed explanation of the objective function and the restrictions involved. Section III outlines the computation outcomes and analysis while implementing the suggested model on the modified IEEE 33-node distribution grid, whereas Section IV presents the findings and potential areas for further study.

II. METHODOLOGY

This section presents a MINLP model for selecting the location and capacity of shunt capacitors. Constraints are considered for the current and security loading conditions. The “~” sign represents the values of variables with the security loading condition.

A. Objective Function

The optimization model aims to minimize the overall expenditures of the electricity distribution network, including both the costs associated with capacitor investments and the costs incurred due to energy loss:

$$\min TC = \sum_{i \in N} z_i \times S_{\text{base}} \times K_C \times Q_{Ci} + \sum_{t=1}^M \left[\sum_{i \in N} 8760 \times \text{LsF} \times c_{\Delta\Delta} \times S_{\text{base}} \times \Delta P_{\text{max}} \right] \times \frac{1}{(1+r)^t} \quad (1)$$

where:

- N stands for the set of buses of the grid;
- z_i is the binary variable, $z_i = 1$ when the capacitor is located at node i , otherwise $z_i = 0$;
- S_{base} is the base power (MVA);
- K_C is the investment cost per kVAr of the compensation capacitor (\$/kVAr);
- Q_{Ci} represents the capacitor size at node i ;
- M is the lifetime of the capacitor;
- t is the index of the time period;
- LsF is the loss factor;
- $c_{\Delta\Delta}$ is the marginal cost of electricity price (\$/kWh);
- ΔP_{max} is the maximum power loss of the power grid;
- r is the discount rate.

B. Constraints of ZIP Load Model

In this study, the ZIP load model was applied to describe the change in power consumption of a load by voltage:

$$P_{Di} = P_{D0i} \times (a_i^p U_i^2 + b_i^p U_i + c_i^p), \quad \forall i \in \Phi_D \quad (2)$$

$$Q_{Di} = Q_{D0i} \times (a_i^q U_i^2 + b_i^q U_i + c_i^q), \quad \forall i \in \Phi_D \quad (3)$$

$$\tilde{P}_{Di} = (1 + \mu_D) \times P_{D0i} \times (a_i^p \tilde{U}_i^2 + b_i^p \tilde{U}_i + c_i^p), \forall i \in \Phi_D \quad (4)$$

$$\tilde{Q}_{Di} = (1 + \mu_D) \times Q_{D0i} \times (a_i^q \tilde{U}_i^2 + b_i^q \tilde{U}_i + c_i^q), \forall i \in \Phi_D \quad (5)$$

where:

- P_{D0i} and Q_{D0i} denote the real and reactive powers of the current demand at node i at the nominal voltage, respectively;
- P_{Di} and Q_{Di} represent the real and reactive powers of the current demand at bus i at the voltage U_i ;
- \tilde{P}_{Di} and \tilde{Q}_{Di} stand for the real and reactive powers of the demand at node i in case of the security loading condition;
- μ_D is loading level;
- U_i denotes the voltage magnitude at bus i for the current loading condition;
- \tilde{U}_i denotes the voltage magnitude at bus i for the security loading condition;
- Φ_D is the set of load demand nodes;
- $a_i^p, b_i^p, c_i^p, a_i^q, b_i^q, c_i^q$ are the coefficients of the ZIP load model, where $a_i^p + b_i^p + c_i^p = 1$ and $a_i^q + b_i^q + c_i^q = 1$.

C. Constraints of Power Balance Equations

The constraints of power balance equations, which relate to corresponding to current and security (critical) loading conditions are described as follows:

$$\sum_{j=1, j \neq i}^N P_{ij} = \sum_{j=1, j \neq i}^N g_{ij} U_i^2 - U_i U_j (g_{ij} \cos \delta_{ij} + b_{ij} \sin \delta_{ij}) = P_{Gi} - P_{Di}, \quad \forall i \in N \quad (6)$$

$$\sum_{j=1, j \neq i}^N Q_{ij} = \sum_{j=1, j \neq i}^N -b_{ij} U_i^2 - U_i U_j (g_{ij} \sin \delta_{ij} - b_{ij} \cos \delta_{ij}) = Q_{Gi} - Q_{Di} + Q_{Ci}, \quad \forall i \in N \quad (7)$$

$$\tilde{P}_{Gi} = (1 + \mu_D + \lambda_G) P_{Gi}, \quad \forall i \in N \quad (8)$$

$$\sum_{j=1, j \neq i}^N \tilde{P}_{ij} = \sum_{j=1, j \neq i}^N g_{ij} \tilde{U}_i^2 - \tilde{U}_i \tilde{U}_j (g_{ij} \cos \tilde{\delta}_{ij} + b_{ij} \sin \tilde{\delta}_{ij}) = \tilde{P}_{Gi} - \tilde{P}_{Di}, \quad \forall i \in N \quad (9)$$

$$\sum_{j=1, j \neq i}^N \tilde{Q}_{ij} = \sum_{j=1, j \neq i}^N -b_{ij} \tilde{U}_i^2 - \tilde{U}_i \tilde{U}_j (g_{ij} \sin \tilde{\delta}_{ij} - b_{ij} \cos \tilde{\delta}_{ij}) = \tilde{Q}_{Gi} - \tilde{Q}_{Di} + Q_{Ci}, \quad \forall i \in N \quad (10)$$

where:

- P_{Gi} and Q_{Gi} are the real and reactive powers of the DG units at node i for the current loading condition, respectively;
- \tilde{P}_{Gi} and \tilde{Q}_{Gi} denote the real power and reactive power produced by DG units at node i for the security loading condition, respectively;
- P_{ij} and Q_{ij} stand for the real and reactive power flows on the branch ij for the current loading condition, respectively;
- \tilde{P}_{ij} and \tilde{Q}_{ij} represent the active and reactive powers flowing through the edge ij for the security loading condition, respectively;
- λ_G is a scalar variable representing the power loss in the security loading condition;
- g_{ij} and b_{ij} denote the real and imaginary elements of the branch susceptance ij , respectively;
- δ_{ij} and $\tilde{\delta}_{ij}$ are the difference of phase angles of voltages at buses i and j for the current and security loading conditions.

D. Constraints of the DG's Output

In this paper, the distributed generating units are modeled as the constant power, i.e., the active power P_{DGi} and reactive power Q_{DGi} of these units are both known. The relationship between the real power and the reactive power of the DG unit at bus i is determined as follows:

$$Q_{DGi} = \frac{P_{DGi} \sqrt{1 - (\cos \varphi_i)^2}}{\cos \varphi_i}, \forall i \in \Phi_{DG} \quad (11)$$

where:

- $\cos \varphi_i$ is the operating power factor of the DG unit at bus i ;
- Φ_{DG} denotes the set of DG units.

E. Limit of the Total Number of Capacitor Locations Installed

The limit on the quantity of capacitor positions deployed on the electrical grid is represented as follows:

$$\sum_{i=1}^N z_i \leq K \quad (12)$$

where K stands for the total number of shunt capacitor installation positions in the power grid (constant).

F. Limit of the Capacitor Size Installed

The bounds of the compensation capacitor size are determined as follows:

$$z_i Q_{Ci}^{\min} \leq Q_{Ci} \leq z_i Q_{Ci}^{\max}, \forall i \in N \quad (13)$$

where Q_{Ci}^{\min} and Q_{Ci}^{\max} denote the minimal and maximal power values of the capacitors.

In this study, the capacity of capacitors is limited: $Q_{Ci}^{\min} = 50 \text{ kVAr}$ and $Q_{Ci}^{\max} = 1000 \text{ kVAr}$.

G. Constraints of Branch Limits

The transmission limits on the branches corresponding to the current and the security loading conditions are given:

$$P_{ij}^2 + Q_{ij}^2 \leq (S_{ij}^{\max})^2, \forall ij \in \Phi_L \quad (14)$$

$$\tilde{P}_{ij}^2 + \tilde{Q}_{ij}^2 \leq (S_{ij}^{\max})^2, \forall ij \in \Phi_L \quad (15)$$

where:

- S_{ij}^{\max} is the maximum transmission power on branch ij ;
- Φ_L is the set of branches of the grid.

H. Limits of the Magnitude and Phase Angle of Nodal Voltage

The constraints of the magnitudes and phase angles of nodal voltages pertaining to the current and security loading conditions are represented as follows:

$$U_i^{\min} \leq U_i \leq U_i^{\max}, \forall i \in N \quad (16)$$

$$\delta_i^{\min} \leq \delta_i \leq \delta_i^{\max}, \forall i \in N \quad (17)$$

$$\tilde{U}_i^{\min} \leq \tilde{U}_i \leq \tilde{U}_i^{\max}, \forall i \in N \quad (18)$$

$$\tilde{\delta}_i^{\min} \leq \tilde{\delta}_i \leq \tilde{\delta}_i^{\max}, \forall i \in N \quad (19)$$

where:

- U_i and δ_i are the magnitude and phase angle of voltage at node i for the current loading condition, respectively;
- \tilde{U}_i and $\tilde{\delta}_i$ represent the magnitude and phase angle of voltage at node i for the security loading condition;
- U_i^{\min} and U_i^{\max} are the lower and upper bounds of voltage magnitude at node i ;
- δ_i^{\min} and δ_i^{\max} stand for the minimal and maximal allowed values of phase angle of voltage at node i , respectively.

I. Constraint of Minimum Loading Level

The minimum loading level constraint that ensures the proper distance between the points of the current operation and the voltage collapse or the closet operating limit is represented as follows:

$$\mu_D \geq \mu_D^{\min} \quad (20)$$

where μ_D^{\min} is the pre-specified minimum value of μ_D .

J. Constraint of Reference Bus Phase Angle

The phase angles of the reference node related to the current and security loading level are constrained by the following expressions:

$$\delta_i = 0, i = ref \tag{21}$$

$$\tilde{\delta}_i = 0, i = ref \tag{22}$$

III. RESULTS AND DISCUSSIONS

In this section, the developed MINLP model is validated using an IEEE 33-bus electrical distribution network [17] on a 2.59-GHz Intel Core i7-8850H computer and 16 GB of RAM. The influence of the minimum loading levels, load models, and DG's operating power factors on the optimal location and capacity of shunt compensation capacitors is examined in detail. The MINLP model is programmed with the GAMS language and solved using the KNITRO commercial solver [18]. The calculation time is 10 seconds, with the optimal gap of the solution accuracy set to 0%.

A. Data Description

Figure. 1 depicts the structure of the modified IEEE power distribution network of 33 nodes. The nominal voltage of this grid is 12.66 kV. The four DG units located at nodes 18, 22, 25, and 33 have the same active power output of 200 kW. The calculation data are presented in Table 2 and Table 3.

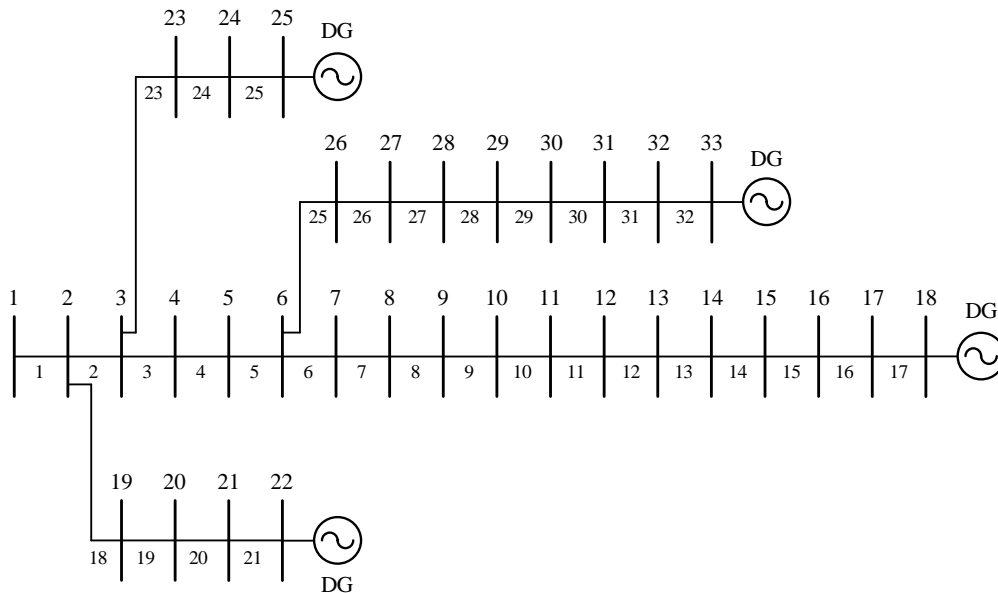


Figure. 1: Modified IEEE 33-node grid

Table 2: Values of computational parameters

Parameter	Value	Unit
K_c	3	\$/kVAr
c_{AA}	0.06	\$/kWh
r	7	%
M	5	year
LsF	0.4	
K	5	
U_i^{\min}	0.94	pu
U_i^{\max}	1.06	pu
S_{base}	10	MVA
U_l	1.06	pu

Table 3: Parameters of the ZIP load model

Load Type	Bus	Coefficients of the ZIP Load Model [19]	
Residential	2, 5, 12, 14, 19, 22, 31, 32	$a_p = 0.24; b_p = 0.62;$ $c_p = 0.13$	$a_Q = 2.44; b_Q = -1.94;$ $c_Q = 0.50$
Commercial	4, 7, 8, 10, 11, 13, 15, 17, 20, 23, 24, 25, 26, 28, 29, 30, 33	$a_p = 0.16; b_p = 0.80;$ $c_p = 0.04$	$a_Q = 3.26; b_Q = -3.10;$ $c_Q = 0.84$
Industrial	3, 6, 9, 16, 18, 21, 27	$a_p = -0.07; b_p = 0.24;$ $c_p = 0.83$	$a_Q = 1.00; b_Q = 0;$ $c_Q = 0$

B. Effect of the Minimum Loading Level

This subsection presents the effect of the minimum loading level μ_D^{\min} on the optimization of the location and size of the shunt compensation capacitors with the ZIP load model. Moreover, the on-site generations operate with a power factor of 0.95 (lagging). Different values of μ_D^{\min} considered are 120%, 130%, and 140%. The solution of the proposed optimization model is presented in Table 4.

Table 4 shows that the capacitor site varies as the minimum loading value μ_D^{\min} change. In particular, capacitors are installed at nodes 7, 14, 17, and 30 with $\mu_D^{\min} = 120\%$; at nodes 14, 18, 30, and 32 with $\mu_D^{\min} = 130\%$; at nodes 14, 18, 30, and 31 with $\mu_D^{\min} = 140\%$. In addition, when factor μ_D^{\min} increases, the size of the invested capacitor also increases (from 1,736.4 kVAr with $\mu_D^{\min} = 120\%$ to 2,204.5 kVAr with $\mu_D^{\min} = 140\%$), thereby leading to an increase in the capital investment of the capacitors (from \$5,208.9 corresponding to $\mu_D^{\min} = 120\%$ to \$6,613.5 for $\mu_D^{\min} = 140\%$). Meanwhile, reactive power compensation to satisfy the node voltage constraint in the condition of security loading can result in a growth in the grid power loss in the current loading condition, which in turn contributes to an increase in the power loss cost as well, increasing from \$66,395 with $\mu_D^{\min} = 120\%$ to \$83,503.6 with $\mu_D^{\min} = 140\%$.

Table 4: The effect of the minimum loading level

μ_D^{\min} (%)	Nodes for capacitor installation	Capacitor size (kVAr)	Investment cost (\$)	Cost of energy loss (\$)	Objective function (\$)
120	7	471.1	5,208.9	66,395	71,604
	14	228			
	17	140.2			
	30	897.1			
130	14	516	5,474.7	73,130.5	78,605.2
	18	158.5			
	30	818			
	32	332.4			
140	14	610.4	6,613.5	83,503.6	90,117.1
	18	215.8			
	30	741.7			
	31	636.6			

The voltage profile of the power grid with three scenarios of the minimum loading level in the current and security (critical) loading conditions is shown in Figure. 2, Figure 3, and Figure 4.

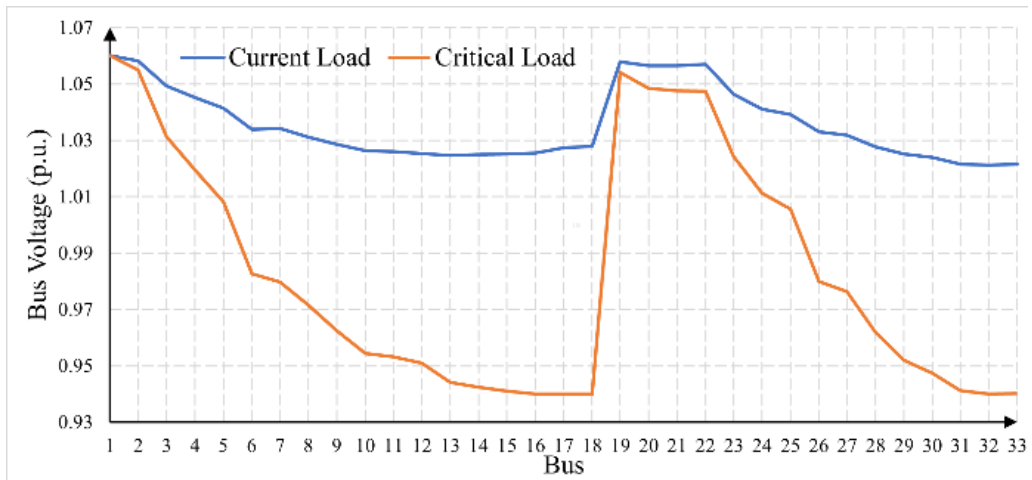


Figure 2: Nodal voltage profile with $\mu_D^{\min} = 120\%$

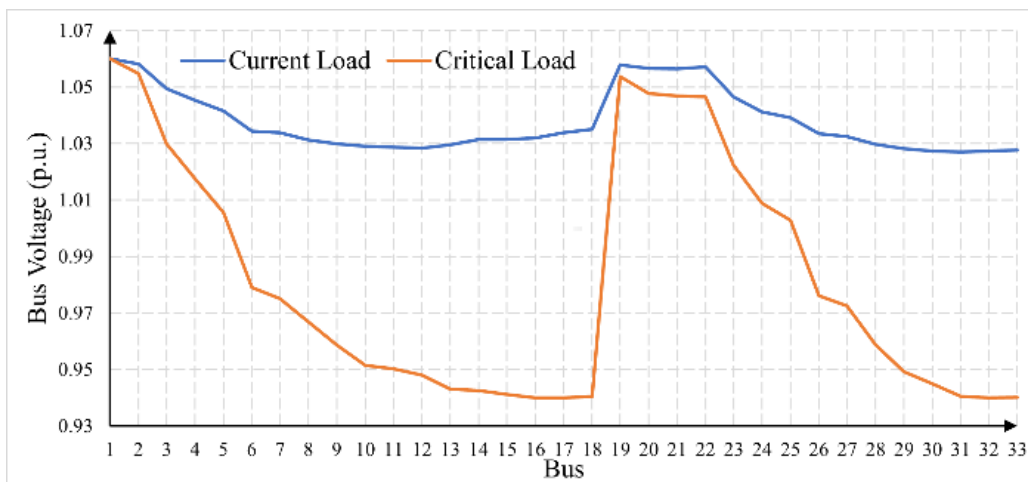


Figure 3: Nodal voltage profile with $\mu_D^{\min} = 130\%$

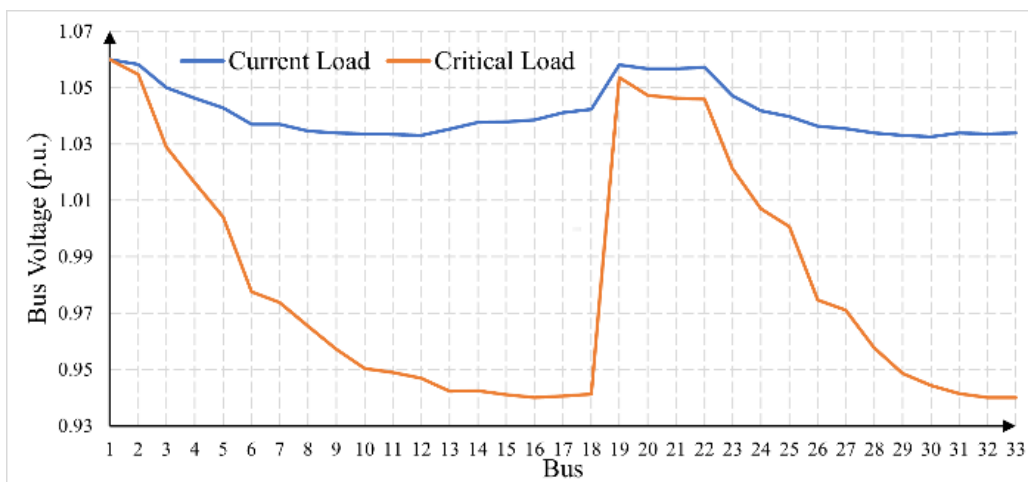


Figure 4: Nodal voltage profile with $\mu_D^{\min} = 140\%$

The calculation results from these graphs show that, for each different minimum loading value, the nodal voltage profile of the test grid will also be distinct:

- Under the scenario $\mu_D^{\min} = 120\%$, the lowest voltage in the current loading condition is 1.02125 pu at node 32; the lowest voltage in the security loading condition is 0.94 pu at buses 16, 18, and 32;
- Under the scenario $\mu_D^{\min} = 130\%$, the lowest voltage in the current loading condition is 1.02692 pu at node 31; the lowest voltage in the security loading condition is 0.94 pu at nodes 16 and 32;

- Under the scenario $\mu_D^{\min} = 140\%$, the lowest voltage in the current loading condition is 1.03249 pu at node 30; the lowest voltage in the security loading condition is 0.94 pu at buses 16 and 32. Furthermore, Figure 5 and Figure. 6 compare the voltage pattern of the grid with three scenarios of minimal loading level for the current and security loading conditions, respectively.

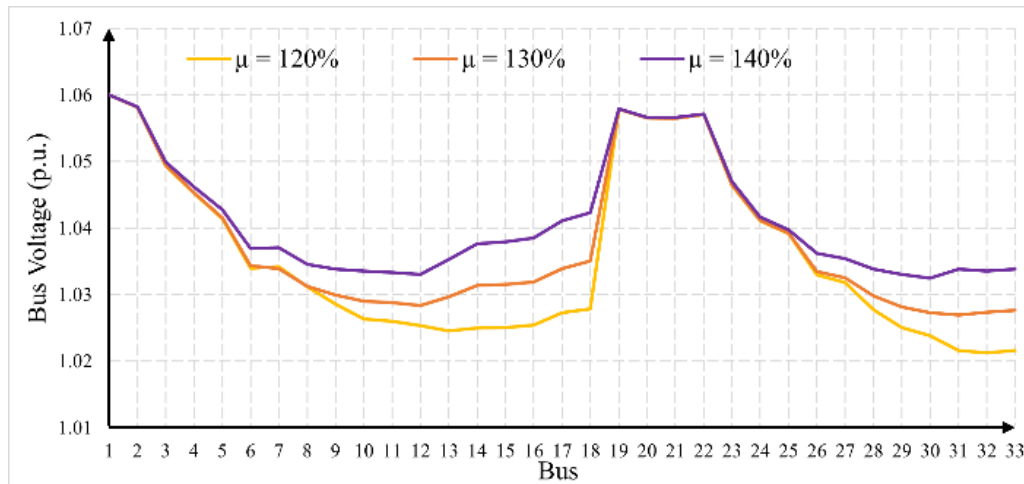


Figure 5: Voltage profile with three different values of the minimal loading level in the current loading condition

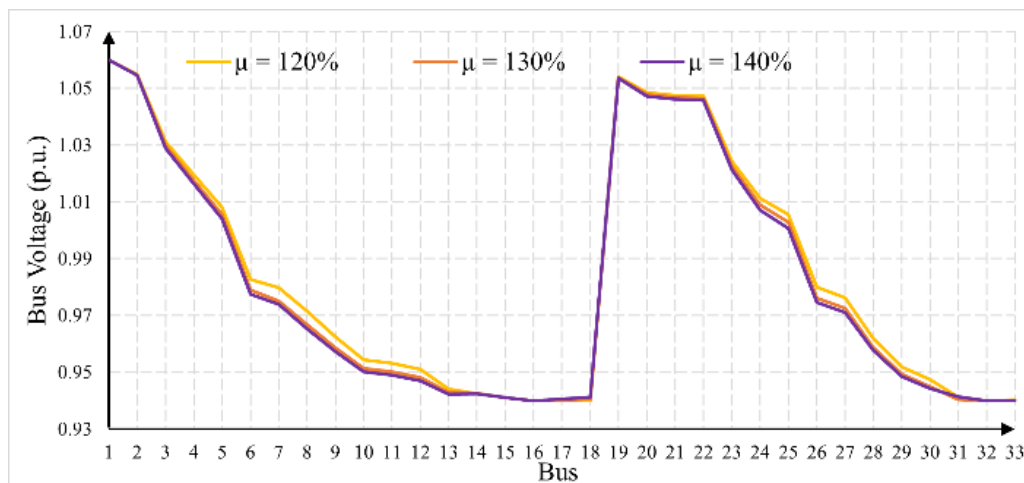


Figure. 6: Voltage profile with three different values of the minimal loading level in the security loading condition

Figure 5 shows that, in the current loading condition, the nodal voltage tends to increase when μ_D^{\min} grows. With $\mu_D^{\min} = 120\%$, the minimum nodal voltage is equal to 1.02125 pu at node 32, while with $\mu_D^{\min} = 140\%$, the lowest nodal voltage is 1.03249 pu at node 31. This is because the power system’s stability margin is increased to guarantee that the nodal voltages remain within the permissible range during the security loading situation.

In the case of the security loading condition (Figure. 6), the lowest nodal voltages in all scenarios have the same value of 0.94 pu.

C. Effect of the Load Model

This subsection presents the influence of the load model on the most suitable placement, along with the size of the shunt capacitors. The two load models under consideration are the constant power model, which represents a load that remains constant, and the voltage-dependent load model, also known as the ZIP load. In addition, the on-site generators run with a power factor of 0.95 (lagging), and the minimum loading level is set to 120%. The computation results when applying the two load forms are presented in Table 5. This table shows that:

- The position and size of the shunt capacitors vary considerably with the load model;

- The total reactive power of the invested capacitors decreases from 2,415.3 kVAr (constant load) to 1,736.4 kVAr (ZIP load). Therefore, the capacitor investment cost with ZIP load is \$2,037.17 lower than that with constant load;
- The cost incurred by the energy loss with the constant load is \$14,647 higher than that with the ZIP load.

Table 5: Effects of load model

Load model	Nodes for capacitor installation	Capacitor size (kVAr)	Investment cost (\$)	Cost of energy loss (\$)	Objective function (\$)
Constant	14	826.3	7,246.07	81,042	88,288.1
	25	220.2			
	30	705.8			
	31	663			
ZIP	7	471.1	5,208.9	66,395	71,604
	14	228			
	17	140.2			
	30	897.1			

Additionally, Figure. 7 and Figure. 8 compare the nodal voltage pattern when applying two load models corresponding to the current and security loading conditions.

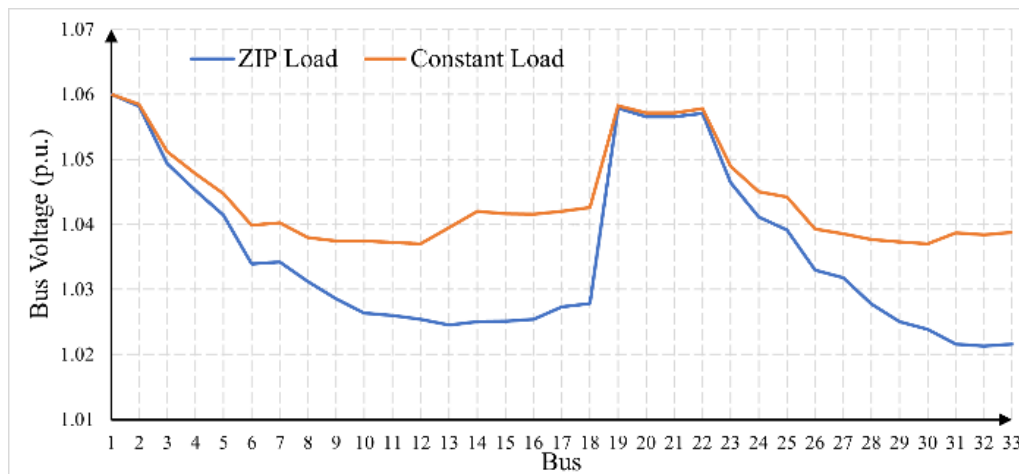


Figure. 7: Voltage profile with two load models in the current loading condition

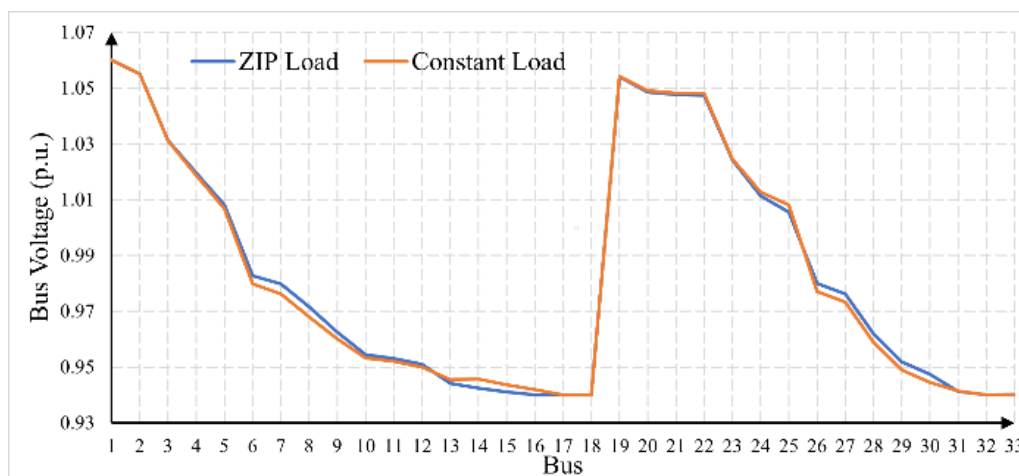


Figure. 8: Voltage profile with two load models in the security loading condition

From these graphs, we can see that:

- In the current loading condition, the nodal voltage with a ZIP load model is lower than that of a constant load model. The lowest voltages for the ZIP and constant load model are 1.02125 pu (at node 32) and 1.037 pu (at node 30), respectively;
- In the security loading condition, the lowest voltage in both load models is 0.94 pu (at nodes 16, 18, and 32 with the ZIP load model and nodes 18 and 32 with the constant load model).

D. Effect of DG’s Operating Power Factor

This subsection presents the effect of the DG’s operational power factor on the optimal position and reactive power of the shunt capacitors. The distinct values of the DG’s operational power factor considered consist of 0.95 (leading), 1, and 0.95 (lagging). The ZIP load model and the minimal loading level of 120% are deployed for evaluation. The optimal solution is given in Table 6.

Table 6: Effect of DG’s operating power factor

Power factor	Nodes for capacitor installation	Capacitor size (kVAr)	Investment cost (\$)	Cost of energy loss (\$)	Objective function (\$)
0.95 (leading)	7	541.9	7,050.7	65,989.4	73,040.1
	17	447.7			
	25	393.9			
	30	711.4			
	32	255.3			
1	7	480.3	6,715.9	66,628.3	73,344.2
	14	554.6			
	25	319.1			
	30	681.3			
	31	203.4			
0.95 (lagging)	7	471.1	5,208.9	66,395	71,604
	14	227.9			
	17	140.2			
	30	897.1			

This table shows that:

- The investment cost and value of the objective function are the lowest when the DG’s operational power factor is 0.95 (lagging), while the expense for energy loss is the lowest when DG units run with the power factor of 0.95 (leading);
- The installed capacitor size is different for each DG’s operational power factor, in which when DG operates with the power factor of 0.95 (lagging), the total reactive power of the invested capacitor is the smallest.

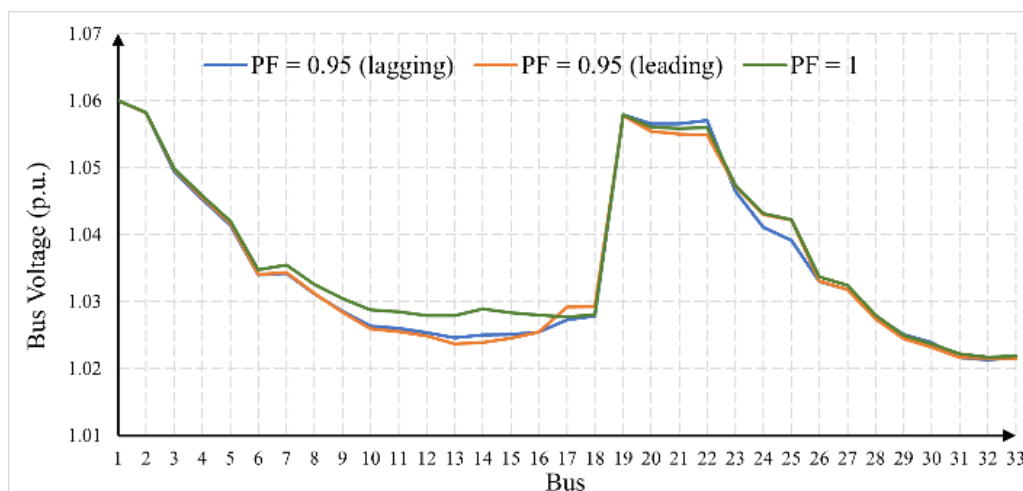


Figure 9: Voltage pattern with three DG’s operational power factor in the current loading condition

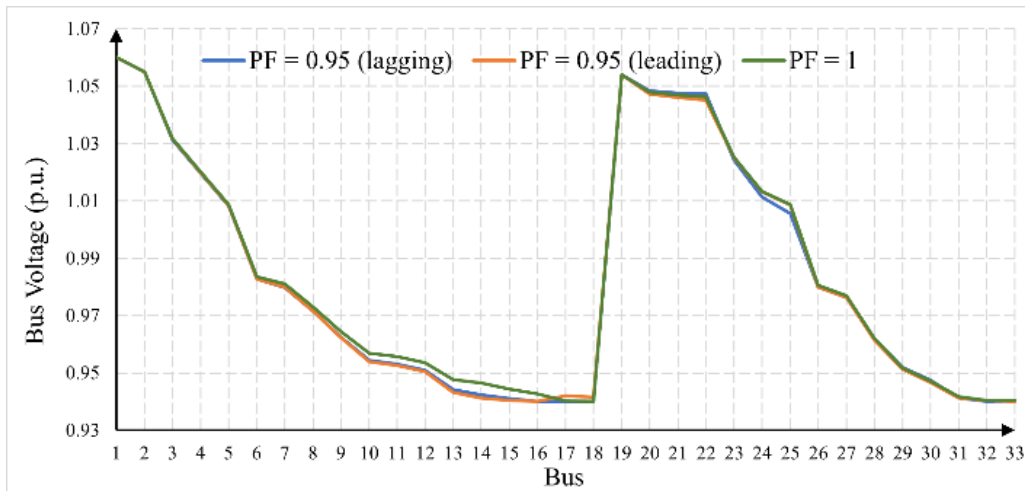


Figure 10: Voltage pattern with three DG's operational power factor in the security loading condition

Figure 9 and Figure 10 illustrate the nodal voltage pattern with the different DG's operational power factors in the current and security loading conditions. Figure 9 shows that in the current loading condition, the minimum nodal voltage of the grid varies with the DG's power factor (1.02148 pu at node 33 with $\cos\varphi=0.95$ (leading); 1.02167 pu at node 32 with $\cos\varphi=1$, and 1.02125 pu at node 32 with $\cos\varphi=0.95$ (lagging)). Figure 10 reveals that in the security loading condition, the lowest voltage of the power grid for all DG's operational power factor is the same as 0.94 pu but corresponds to different nodes (node 16 with $\cos\varphi=0.95$ (leading); node 18 with $\cos\varphi=1$; nodes 16, 18 and 32 with $\cos\varphi=0.95$ (lagging)).

IV. CONCLUSION

This study proposed the optimization model to compute the location and size of shunt compensation capacitors in DG-integrated power distribution grids, taking voltage stability constraints into account. The proposed optimization formulation takes the form of mixed-integer nonlinear programming (MINLP) with the objective function of minimizing total costs, including the investment expense of capacitors and expenditure for energy losses. The influence of the minimum loading level, load model, and operational power factor of on-site generators on the optimal solution is carefully considered. The modified IEEE 33-node electrical distribution grid is deployed to evaluate the proposed optimization model. The calculation findings indicate that the best placement and capacity of shunt capacitors are greatly influenced by voltage stability restrictions, the load model, and the operating mode of the DG units. In addition, the proposed optimization approach is fully applicable to both power distribution grids with meshed structures and power transmission networks. Future work is planned to develop a mixed-integer second-order cone programming (MISOCP) model that accounts for the variation in the load consumption power over time.

REFERENCES

- [1] V. Vita, T. Alimardan, and L. Ekonomou, "The Impact of Distributed Generation in the Distribution Networks' Voltage Profile and Energy Losses," in 2015 IEEE European Modelling Symposium (EMS), Oct. 2015, pp. 260–265. doi: 10.1109/EMS.2015.46.
- [2] J. Modarresi, E. Gholipour, and A. Khodabakhshian, "A comprehensive review of the voltage stability indices," *Renewable and Sustainable Energy Reviews*, vol. 63, pp. 1–12, Sep. 2016, doi: 10.1016/j.rser.2016.05.010.
- [3] L. Chi Kien, T. Thanh Nguyen, T. Minh Phan, and T. Trung Nguyen, "Maximize the penetration level of photovoltaic systems and shunt capacitors in distribution systems for reducing active power loss and eliminating conventional power source," *Sustainable Energy Technologies and Assessments*, vol. 52, p. 102253, Aug. 2022, doi: 10.1016/j.seta.2022.102253.
- [4] S. Nojavan, M. Jalali, and K. Zare, "Optimal allocation of capacitors in radial/mesh distribution systems using mixed integer nonlinear programming approach," *Electric Power Systems Research*, vol. 107, pp. 119–124, Feb. 2014, doi: 10.1016/j.epr.2013.09.019.
- [5] L. W. de Oliveira, S. Carneiro, E. J. de Oliveira, J. L. R. Pereira, I. C. Silva, and J. S. Costa, "Optimal reconfiguration and capacitor allocation in radial distribution systems for energy losses minimization," *International Journal of Electrical Power & Energy Systems*, vol. 32, no. 8, pp. 840–848, Oct. 2010, doi: 10.1016/j.ijepes.2010.01.030.
- [6] Y. Ogita and H. Mori, "Parallel Dual Tabu Search for Capacitor Placement in Smart Grids," *Procedia Computer Science*, vol. 12, pp. 307–313, Jan. 2012, doi: 10.1016/j.procs.2012.09.076.

- [7] M. A. S. Masoum, A. Jafarian, M. Ladjevardi, E. F. Fuchs, and W. M. Grady, "Fuzzy approach for optimal placement and sizing of capacitor banks in the presence of harmonics," *IEEE Transactions on Power Delivery*, vol. 19, no. 2, pp. 822–829, Apr. 2004, doi: 10.1109/TPWRD.2003.823187.
- [8] S. Das, D. Das, and A. Patra, "Operation of distribution network with optimal placement and sizing of dispatchable DGs and shunt capacitors," *Renewable and Sustainable Energy Reviews*, vol. 113, p. 109219, Oct. 2019, doi: 10.1016/j.rser.2019.06.026.
- [9] K. Prakash and M. Sydulu, "Particle Swarm Optimization Based Capacitor Placement on Radial Distribution Systems," in 2007 IEEE Power Engineering Society General Meeting, Jun. 2007, pp. 1–5. doi: 10.1109/PES.2007.386149.
- [10] R. Sirjani, A. Mohamed, and H. Shareef, "Optimal capacitor placement in a distribution network with nonlinear loads using Harmony Search algorithm," *Australian Journal of Basic and Applied Sciences*, vol. 5, pp. 461–474, Jun. 2011.
- [11] M. O. Okelola, O. W. Adebisi, S. A. Salimon, S. O. Ayanlade, and A. L. Amoo, "Optimal sizing and placement of shunt capacitors on the distribution system using Whale Optimization Algorithm," *Nigerian Journal of Technological Development*, vol. 19, no. 1, Art. no. 1, Jun. 2022, doi: 10.4314/njtd.v19i1.5.
- [12] A. Eid and S. Kamel, "Optimal Allocation of Shunt Compensators in Distribution Systems using Turbulent Flow of Waterbased Optimization Algorithm," in 2020 IEEE Electric Power and Energy Conference (EPEC), Oct. 2020, pp. 1–5. doi: 10.1109/EPEC48502.2020.9320085.
- [13] B. Das and P. K. Verma, "Artificial neural network-based optimal capacitor switching in a distribution system," *Electric Power Systems Research*, vol. 60, no. 2, pp. 55–62, Dec. 2001, doi: 10.1016/S0378-7796(01)00149-3.
- [14] V. V. S. N. Murty and A. Kumar, "Capacitor Allocation in Radial Distribution System with Time-Varying ZIP Load Model and Energy Savings," *Procedia Computer Science*, vol. 70, pp. 377–383, Jan. 2015, doi: 10.1016/j.procs.2015.10.039.
- [15] O. M. Neda, "A Novel Technique for Optimal Siting and Rating of Shunt Capacitors Placed to the Radial Distribution Systems," *Advances in Electrical and Electronic Engineering*, vol. 20, no. 2, Jun. 2022, doi: 10.15598/aeec.v20i2.4415.
- [16] M. F. Shaikh, A. M. Shaikh, S. A. Shaikh, R. Nadeem, A. M. Shaikh, and A. A. Khokhar, "Mitigation of Power Losses and Enhancement in Voltage Profile by Optimal Placement of Capacitor Banks With Particle Swarm Optimization in Radial Distribution Networks," *Advances in Electrical and Electronic Engineering*, vol. 20, no. 4, Feb. 2023, doi: 10.15598/aeec.v20i4.4615.
- [17] S. H. Dolatabadi, M. Ghorbanian, P. Siano, and N. D. Hatziargyriou, "An Enhanced IEEE 33 Bus Benchmark Test System for Distribution System Studies," *IEEE Transactions on Power Systems*, vol. 36, no. 3, pp. 2565–2572, May 2021, doi: 10.1109/TPWRS.2020.3038030.
- [18] GAMS [Online]. Available: <https://www.gams.com/>. Accessed: Oct. 11, 2023.
- [19] J. R. Martí, H. Ahmadi, and L. Bashualdo, "Linear Power-Flow Formulation Based on a Voltage-Dependent Load Model," *IEEE Transactions on Power Delivery*, vol. 28, no. 3, pp. 1682–1690, Jul. 2013, doi: 10.1109/TPWRD.2013.2247068.